A New Mammaliaform from the Early Jurassic and Evolution of Mammalian Characteristics

Author(s): Zhe-Xi Luo, Alfred W. Crompton and Ai-Lin Sun

Source: *Science*, New Series, Vol. 292, No. 5521 (May 25, 2001), pp. 1535-1540
Published by: American Association for the Advancement of Science
Stable URL: http://www.jstor.org/stable/3083825
Accessed: 03-04-2017 22:01 UTC

A New Mammaliaform from the Early Jurassic and Evolution of Mammalian Characteristics

Zhe-Xi Luo,[1]* Alfred W. Crompton,[2] Ai-Lin Sun[3]

A fossil from the Early Jurassic (Sinemurian, ~195 million years ago) represents a new lineage of mammaliaforms, the extinct groups more closely related to the living mammals than to nonmammaliaform cynodonts. It has an enlarged cranial cavity, but no postdentary trough on the mandible, indicating separation of the middle ear bones from the mandible. This extends the earliest record of these crucial mammalian features by some 45 million years and suggests that separation of the middle ear bones from the mandible and the expanded brain vault could be correlated. It shows that several key mammalian evolutionary innovations in the ear region, the temporomandibular joint, and the brain vault evolved incrementally through mammaliaform evolution and long before the differentiation of the living mammal groups. With an estimated body weight of only 2 grams, its coexistence with other larger mammaliaforms with similar "triconodont-like" teeth for insectivory within the same fauna suggests a great trophic diversity within the mammaliaform insectivore feeding guild, as inferred from the range of body sizes.

Hadrocodium wui (*1*) from the Lower Lufeng Formation of Yunnan, China, is distinguishable from all other nonmammalian mammaliaforms (*2–14*) and mammals from the Late Triassic and Jurassic in a long list of dental (*15*) and derived skull characteristics (Figs. 1, 2, and 3). The holotype specimen of *Hadrocodium* displays several features typical of adults or subadults of late growth stages of other mammaliaforms and living mammals. The first adult feature is its large postcanine diastema, the gap between the functional canine and the first premolar (Fig. 1). A prominent postcanine diastema is characteristic of older individuals of *Sinoconodon* (*14*), *Morganucodon* (*9–12*), and *Kuehneotherium* (*8*, *12*), in which the anteriormost premolars are present in the smaller and younger individuals but lost without being replaced in the larger and adult individuals. *Hadrocodium*'s postcanine diastema is very large relative to the postcanine row, similar to adults of the late stages, but very different from the young individuals of *Sinoconodon* (*14*) and *Morganucodon* (*12*). The second adult feature of *Hadrocodium* is the presence of wear facets on the molars (Fig. 1, D and E), showing that it had grown to a later stage of independent feeding. The third adult feature is a fully functioning temporomandibular joint (TMJ), which only appears beyond the suckling stage of early growth in extant monotremes (*16–18*) and therians (*19–21*). The fourth feature is the absence of the meckelian sulcus in the mandible of *Hadrocodium* (Fig. 3D). In living mammals, this sulcus is lost in the adult after the reabsorption of the anterior part of the Meckel's cartilage, which would be associated with the meckelian sulcus on the dentary during embryonic stages (*16–21*). These adult features indicate that the type specimen of *Hadrocodium* had undoubtedly developed beyond the early juvenile stages of living mammals. Its extremely small size is unlikely to be due to accidental sampling of an early ontogenetic stage. Its distinctive features are of phylogenetic importance.

Hadrocodium is the sister taxon to the clade of triconodontids and extant Mammalia (Fig. 4), based on the parsimony analysis of 90 cranial and dental characters that can be recognized on its type specimen (*22*). Among 15 comparative taxa, it is more closely related to living mammals than are *Adelobasileus*, *Sinoconodon*, morganucodontids, and *Haldanodon*. The sister taxon relationship of *Hadrocodium* to the clade of triconodontids and living mammals is supported by a large number of shared derived characters (Fig. 4B, node 6).

The first suite of apomorphies is on the medial side of the mandible of *Hadrocodium*, which has a smooth periosteal surface but lacks the postdentary trough and its medial ridge, and lacks the medial concavity of mandibular angle (Fig. 3). By contrast, more primitive morganucodontids (*9–14*), kuehneotheriids (*8*), *Haramiyavia* (*6*), and *Haldanodon* (*22*) have a very prominent postdentary trough with a shelflike dorsal medial ridge, and all other nonmammalian mammaliaforms have a medial concavity on the mandibular angle (*8–14*, *23*), as in nonmammaliaform cynodonts (*9*, *14*, *24–27*). The postdentary trough and the medial concavity on the mandibular angle respectively accommodated the prearticular/surangular and the reflected lamina of the angular (*9*, *25–27*) that are the homologs to the mammalian middle ear bones (*9*, *14*, *16–21*, *23*, *26*). The absence of these structures indicates that the postdentary bones ("middle ear ossicles") must have been separated from the mandible (Fig. 3). *Hadrocodium* lacks the primitive meckelian sulcus of the mandible typical of all nonmammaliaform cynodonts (*24–27*), stem groups of mammaliaforms (*8*, *9*, *14*, *23*, *26*, *27*), triconodontids (*28*, *29*), and nontribosphenic therian mammals (*30*). *Hadrocodium* differs from all other stem mammaliaforms and most mammals in having a slightly inflected dentary angle, which is an autapomorphy (Fig. 1B).

The second suite of derived features is related to the enlargement of the brain in *Hadrocodium* (Fig. 3). Its cranial vault is wider and more expanded in the alisphenoid and parietal region than those of all other nonmammalian mammaliaforms (*7*, *10*, *14*, *23*) and all other Jurassic mammals (*31–34*) known to this date. The brain vault in the parietal region in *Hadrocodium* is comparable to those of the mammalian crown group (*31–34*), but wider than in nonmammaliaform cynodonts (*24*, *25*), *Sinoconodon* (*14*), *Morganucodon* (*10*, *33*), and *Haldanodon* (*23*) (Fig. 3). On the basis of the allometric scaling of a large sample of living and fossil mammals, the brain vault of *Hadrocodium* is larger than expected for the mammals of its comparable skull width (Fig. 5A) and far wider than in any other Triassic-Jurassic mammaliaforms. Our scaling analysis shows that the small size of *Hadrocodium*, in and by itself, is not sufficient to explain its large brain (Fig. 5A). Related to the expansion of the brain vault, the cerebellar portion of the brain cavity is expanded more posteriorly than the level of TMJ (Figs. 1A and 3D). The occipital (posterior) wall of the brain cavity is convex posteriorly beyond the lambdoidal crest (Fig. 1A), instead of concave or flat as in cynodonts, other mammaliaforms, and all Jurassic mammals known to this date (*7*, *10*, *14*, *23–27*).

The third suite of derived features of *Hadrocodium* is in the TMJ. All other nonmammalian mammaliaform crania have a TMJ positioned in about the same transverse level as the fenestra vestibuli and occipital condyles (*10*, *14*, *23*, *27*). By contrast, in *Hadrocodium*, the zygoma swings anteriorly from the cranial moiety of the squamosal, and the TMJ is positioned anterior to the level of

[1]Section of Vertebrate Paleontology, Carnegie Museum of Natural History, Pittsburgh, PA 15213, USA. [2]Museum of Comparative Zoology, Harvard University, Cambridge, MA 02138, USA. [3]Institute of Vertebrate Paleontology and Paleoanthropology, Chinese Academy of Sciences, Beijing 100044, China.

*To whom correspondence should be addressed. E-mail: luoz@carnegiemuseums.org

the fenestra vestibuli and to occipital condyles (Fig. 2), in correlation with the expanded brain vault. A postglenoid depression is present on the lateral aspect of the squamosal between the zygoma and the cranial moiety. These are derived characteristics of some eutriconodonts (*29*), many multituberculates (*35*, *36*), the monotremes *Obdurodon* (*37*) and *Tachyglossus* (*16*), and the majority of therian mammals (*19*–*21*). *Hadrocodium* has a well-developed postglenoid region behind the TMJ (Fig. 2), in correlation with the posterior displacement of the basicranium and brain vault behind the TMJ. A similar pattern appears to be correlated with the detachment of the middle ear from the mandible in *Monodelphis* (*33*).

The fourth suite of derived features of *Hadrocodium* is in the petrosal (Fig. 2). The petrosal has a prominent promontorium (bony housing of the inner ear cochlea), more inflated than those of other mammaliaforms (*7*, *10*, *14*, *23*, *38*), triconodontids (*39*, *40*), most multituberculates (*35*, *36*, *40*), and nontribosphenic therians (*30*). The large promontorium may be inversely correlated to the small size of the skull, as the inner ear may have negative allometry with the skull size. A shallow epitympanic recess, the location for attachment of the incus, is on the lateral side of the well-developed crista parotica, more derived than the condition of *Morganucodon* (*41*), but similar to the conditions of *Tachyglossus* and multituberculates. The recess lacks the distinctive incus fossa of *Ornithorhynchus* (*18*, *40*, *41*) and some triconodontids (*39*, *40*); it is more posteriorly positioned relative to the TMJ than in these taxa. It is likely that *Hadrocodium* already developed a mobile articulation of the quadrate (incus) to the cranium, as in derived cynodonts (*26*), other mammaliaforms (*41*), and living mammals. The pterygoparoccipital foramen for the superior ramus of the stapedial artery in *Hadrocodium* is completely enclosed by the petrosal, different from most mammaliaforms (*38*–*41*) (Fig. 2) but similar to those in monotremes and multituberculates. The paroccipital process of the petrosal lacks the bifurcating pattern common to *Sinoconodon*, morganucodontids, triconodontids, and some advanced cynodonts (*38*, *42*). It lacks the ventrally projecting posterior paroccipital process seen in morganucodontids, triconodontids, multituberculates, and *Ornithorhynchus*.

The bony roof of the oropharyngeal passage is broad, flat, and almost featureless. There are no constriction between the pterygoid and the basisphenoid, no pterygopalatine ridges, and no median ridge of the basisphenoid (Figs. 1B and 2C), all of which are primitive characters of nonmammaliaform cynodonts (*24*, *25*), *Sinoconodon*, *Morganucodon*, and *Megazostrodon* and are present, although less developed, in *Adelobasileus* (*7*) and multituberculates (*35*, *36*). The small hamulus of the pterygoid is similar to the condition in *Haldanodon*, *Ornithorhynchus*, and multituberculates but more reduced than the homologous transverse flange of cynodonts (*24*, *25*), *Sinoconodon*, and *Morganucodon* (*14*). The posterior edge of the secondary bony palate (partially broken) lies posterior to the tooth row, more derived than in *Sinoconodon*, *Morganucodon*, and multituberculates but less than in *Haldanodon* (*23*), eutriconodonts, and the mammalian crown group taxa.

Our phylogeny shows that all cranio-dental diagnostic characters for the extant Mammalia evolved stepwise (*27*) and before the diversification of the extant mammalian clades (node 8 in Fig. 4B). The transformation from a more complex "double jaw hinge" (of the articular-quadrate and dentary-squamosal in *Sinoconodon*, *Morganucodon*, and *Haldanodon*) to the "single jaw hinge" joint (TMJ) (formed exclusively of the dentary-squamosal in *Hadrocodium*, triconodontids, and extant mammals) be-

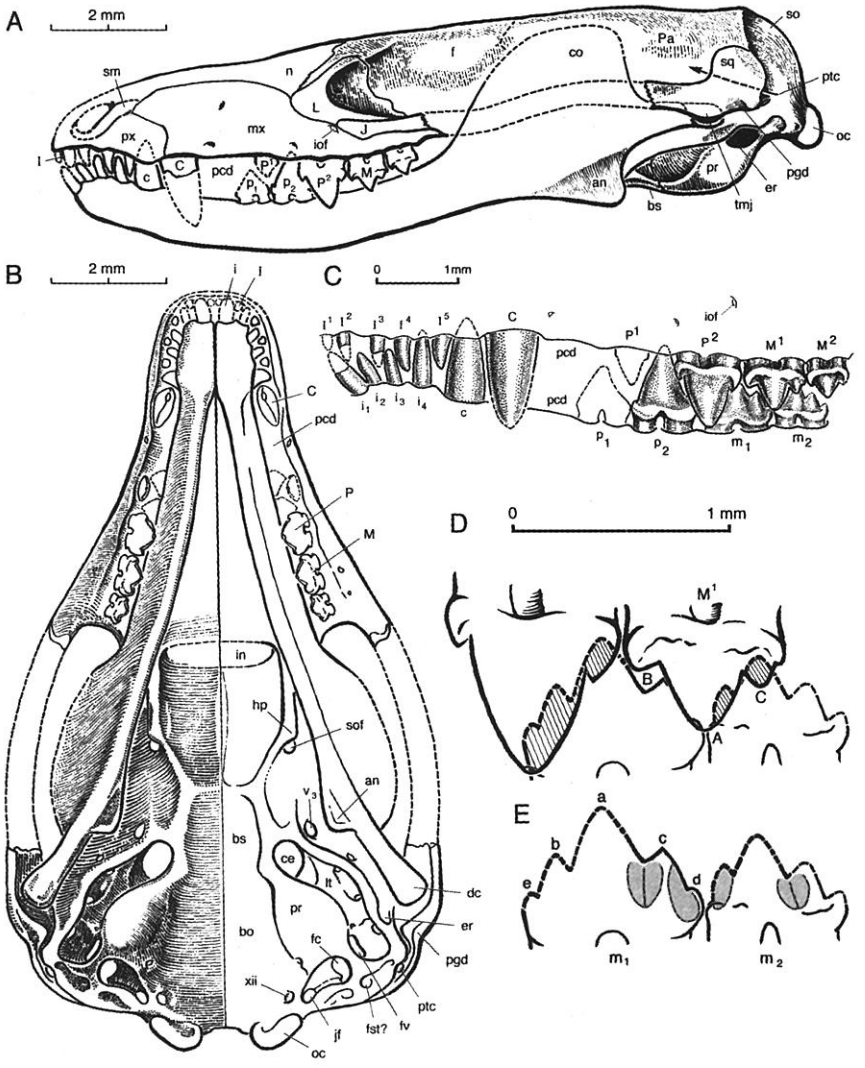

Fig. 1. *Hadrocodium wui gen. et sp. nov.* (IVPP 8275). (**A**) Lateral and (**B**) ventral views of restored skull. (**C**) Dentition (lateral view restoration). (**D**) Occlusion [based on scanning electron microscope (SEM) photos]. (**E**) Wear of molars (shaded areas are wear facets). The main cusp A of the upper molar occludes in the embrasure between the opposite lower molars. Abbreviations.: an, angular process (dentary); bo, basioccipital; bs, basisphenoid; c, canine; ce, cavum epiptericum; co, coronoid process (of dentary); dc, dentary condyle; er, epitympanic recess; f, frontal; fc, foramen cochleare ("perilymphatic foramen"); fst, fossa for stapedial muscle; fv, fenestra vestibuli; hp, hamulus (of pterygoid); I/i, upper and lower incisors; in, internal nares; iof, infraorbital foramen; J, jugal; jf, jugular foramen; L, lacrimal; lt, lateral trough; M, molar; mx, maxillary; n, nasal; oc, occipital condyle; P, premolar; Pa, parietal; pcd, postcanine diastema; pgd, postglenoid degression; pr, promontorium (petrosal); ptc, posttemporal canal (between petrosal and squamosal); px, premaxillary; sm, septomaxillary; so, supraoccipital; sof, spheno-orbital fissure; sq, squamosal; tmj, temporomandibular joint (dentary/squamosal jaw hinge); v3, foramen for the mandibular branch of the trigeminal nerve (v); xii, hypoglossal nerve (xii). Molar cusps following (*11*): A, B, and C, main cusps of upper molars; a, b, c, d, and e, cusps of the lowers.

gan in node 1 and was completed in node 3 (Fig. 4B). The promontorium of the petrosal pars cochlearis was incipient in node 2 and fully developed in node 4. A mammal-like incus suspension for the middle ear occurs in node 4 (*41*), but complete separation of the middle ear from the mandible did not occur until node 6. The expansion of the brain vault (*33*, *34*), possibly related to the development of the neocortex (*33*, *34*), occurs before the divergence (Fig. 4B; node 6) of *Hadrocodium*, triconodontids, and extant mammals.

The acquisition of "mammalian characteristics" shows an additive pattern in our mammaliaform phylogeny (Fig. 4C). The transition from the nonmammaliaform cynodonts to living mammals has a stepwise and incremental acquisition of the mammalian characteristics (*24*–*27*, *43*), and there was no single episode of rapid evolution of a large number of derived characters. The node of crown-group Mammalia [following (*42*)] has four unambiguous synapomorphies, within the range of three to ten unambiguous synapomorphies for each of the internodal segments on the backbone of the cladogram. This is consistent with a macroevolutionary pattern that prevailed in much of synapsid evolution (*24*, *25*, *43*).

Hadrocodium sheds light on evolution of the mammalian middle ear. It is the earliest known taxon that lacks the primitive attachment of the middle ear bones to the mandible but has an enlarged brain vault (suggestive of a large brain) (Fig. 5A). This extends the first appearance of these modern mammalian features back to the Early Jurassic, some 45 million years earlier than the next oldest mammals that have preserved such derived features, such as *Triconodon* from the Late Jurassic (*31*–*34*). All other nonmammalian mammaliaforms with small brain vaults (Fig. 3, A to C) have retained the mandibular attachment of the middle ear bones, whereas *Hadrocodium* and living mammals (Fig. 3, D to I) with larger brain vaults have lost the mandibular attachment to the middle ear.

During the ontogeny of the marsupial *Monodelphis*, the chain of middle ear ossicles and the ectotympanic ring ossify and terminate their growth in size earlier than does the brain (*33*). In subsequent development, the ossicles and the ectotympanic ring, with their size fixed upon ossification, show negative allometry relative to the increasing size of the brain, the basicranium, and the entire skull. Negative allometry of the middle ear bones during development is known for monotremes (*17*, *44*) and some placentals (*21*). Negative allometry of adult middle ear bones occurs in diverse placental (*45*) and some marsupial (*19*) taxa of a wide range of body sizes.

Given this negative allometry of the middle ear ossicles and that the ossicles are connected to the basicranium through the fenestra vestibuli (*33*) and bound by connective tissues to the crista parotica (*19*, *21*, *41*), the peramorphic growth of the brain and the basicranium would cause the ectotympanic ring to move away from the mandibular angle, as the distance increases between the mandible and the crista parotica and fenestra vestibuli. The detachment of the ectotympanic ring from the mandible is in part correlated with the peramorphic growth of the brain (*33*) and the posterior displacement of the basicranium (Fig. 3). This may provide a mechanism that could have separated the middle ear (*33*), a crucial step in transforming the mandibular elements for feeding to the middle ear structures specialized for hearing (*16*–*21*, *26*). The concurrence of the expanded brain vault and the separation of the middle ear from the mandible in *Hadrocodium* (Fig. 3) is consistent with the observed correlation of the peramorphic growth of brain and basicranium to the separation of the middle ear bones from the mandible during development (*33*).

Correlation of negative allometry of the middle ear elements to the peramorphic growth of the brain should be tested by further comparative studies of developmental rates that are

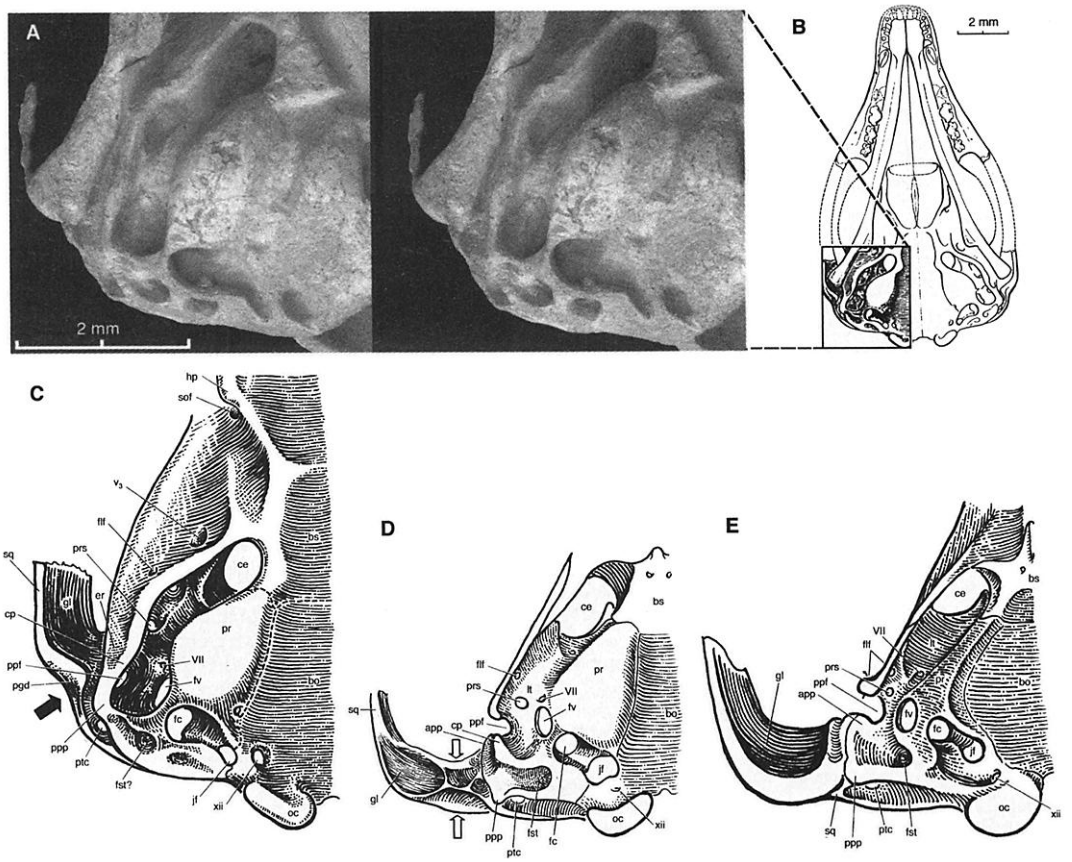

Fig. 2. Ear regions of some early mammaliaforms. (**A** and **B**) Skull and ear region (SEM photographs of right basicranium with slight distortion) of *Hadrocodium*. The squamosal and the occipital condyles are submerged in the wax (black background) to secure the specimen for SEM. (**C**) *Hadrocodium* (restoration without dentary); solid arrow shows postglenoid depression and the anterior placement of TMJ. (**D**) *Morganucodon* [after (*10*, *27*, *38*)]. Light arrows show squamosal constriction. (**E**) *Sinoconodon*. Abbreviations: app, anterior paroccipital process; bo, basioccipital; bs, basisphenoid; ce, cavum epiptericum; cp, crista parotica; er, epitympanic recess; fc, foramen cochleae ("perilymphatic foramen"); flf, foramen (vascular) on lateral flange; fst, fossa for stapedial muscle; fv, fenestra vestibuli; gl, glenoid fossa (for TMJ); hp, pterygoid hamulus; jf, jugular foramen; lt, lateral trough; oc, occipital condyle; pgd, postglenoid degression; ppf, ptergoparoccipital foramen (for ramus superior of stapedial artery); ppp, posterior paroccipital process; pr, promontorium; prs, prootic sinus canal; ptc, posttemporal canal; sof, spheno- orbital fissure; sq, squamosal; v3; foramen for the trigeminal mandibular n.; VII, foramen for the facial nerve (VII); xii, hypoglossal nerve (xii).

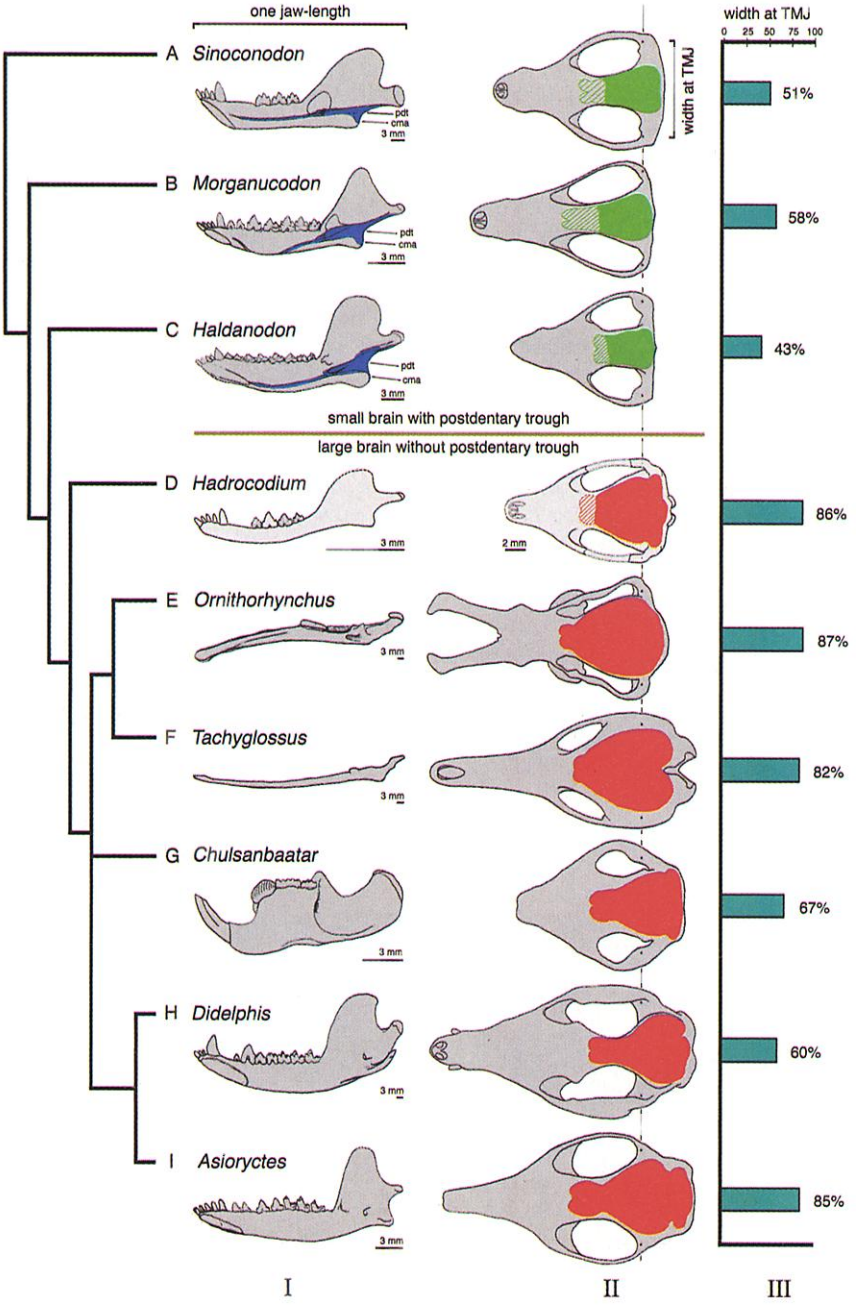

Fig. 3. Correlation of the expanded brain vault and the loss of the postdentary trough and medial concavity of mandibular angle in *Hadrocodium* and more derived mammals. (I, Left) Internal view of dentaries (standardized to one jaw length, scales differ among taxa); the postdentary trough, the medial concavity, and the meckelian sulcus on the mandibular angle are colored in blue. Abbreviations: cma, medial concavity of the mandibular angle; pdt, postdentary trough. (II, Middle) Dorsal view of the cranium (crania of different sizes are standardized to the same width between the left and right temporomandibular joints; scales differ among taxa); the areas in red represent the approximate extent of the brain endocasts. (III, Right) Measurement of the brain vault size (cranial width at the squamosal-parietal suture) relative to the width between the two TMJs; value on bar represents the width of brain vault in percentage of total skull width at the TMJs. *Hadrocodium* (85%) and mammalian crown groups (60% to 87%) with larger brain vaults show the separation of the middle ear ossicles from the mandible. *Hadrocodium* has a larger brain vault than expected for living mammals of its skull size (see allometry regression in Fig. 5B) and is similar to living mammals but different from other contemporaneous mammaliaforms. All primitive mammaliaforms [(A) to (C)] in the basal part of the tree have the postdentary trough and medial concavity of mandibular angle (for postdentary "ear" elements), as well as small brain vault (43 to 58%). The 58% value for *Morganucodon*, although larger than *Haldanodon* and *Sinoconodon*, is far below the ~75% expected for extant mammals of similar skull size (Fig. 5A). (**A**) *Sinconodon*. (**B**) *Morganucodon*. (**C**) *Haldanodon* [after (*23*)]. (**D**) *Hadrocodium* (brain endocast outline based on the exposed borders on the right side). (**E**) Monotreme *Ornithorhynchus*. (**F**) Monotreme *Tachyglossus*. (**G**) Multituberculate *Chulsanbaatar* [after (*36*)]. (**H**) Marsupial *Didelphis* [after (*33*)]. (**I**) Placental *Asioryctes* [after (*31*)].

known to differ in various parts of the skull among marsupial species (*46*). Marsupials, monotremes, and placentals differ in the developmental rates and timing of skull components relative to the central nervous system (*46*, *47*) and also in topographic relations of the Meckel's cartilage to the dentary (*20*). Other developmental processes have also been proposed to explain the detachment of the middle ear bones (*19*, *48*, *49*).

The body mass of *Hadrocodium* is estimated to be 2 g from a skull length at 12 mm (Fig. 5B), on the basis of the well-established scaling relationship of body mass to skull size in 64 species of living lipotyphlan insectivore mammals (*50*). This taxon ranks among the smallest mammals (*51*) and is certainly the smallest mammal yet discovered in the Mesozoic. The smallest living insectivoran placental has an adult weight of about 2.5 g. The smallest bat has an adult weight of about 2.0 g (*51*). The smallest Cenozoic fossil insectivore mammal has an estimated body weight of 1.3 to 2.04 g (*51*). The body masses of all other fossil mammals of the Cretaceous and Cenozoic are near or above 3 g (*52*). The diminutive body size of *Hadrocodium* greatly expands the range of body size for the early Jurassic mammaliaform insectivores (Fig. 5B). The morphological disparity (*53*, *54*) within the earliest mammaliaform insectivore guild, as indicated by skull sizes (Fig. 5B), is almost equal to the range of disparity of living lipotyphlan insectivore mammals with diverse trophic adaptations (*50*, *51*). The wide range of body size within the Lufeng mammaliaform fauna suggests a trophic differentiation within the insectivorous mammaliaform feeding guild (Fig. 5B), which is an important paleoecological feature for the early diversification of mammals, in addition to the splitting of phylogenetic clades, as documented elsewhere for the early diversification in some invertebrate groups (*55*) and for later mammals (*52*–*54*).

References and Notes

1. Etymology: *Hadro*, fullness (Greek); *codium*, head (Greek); for its very large brain capacity relative to the skull; *Wui*, after Dr. X.-C. Wu who, in 1985, discovered the holotype IVPP 8275 (Institute of Vertebrate Paleontology and Paleoanthropology, Beijing), a nearly complete skull, 12 mm in rostro-occipital length and 8 mm in width at the level of temporomandibular joint. The unprepared specimen was mentioned as a juvenile morganucodontid (*14*). Now after full preparation, the specimen shows many taxonomic differences from any previously known mammaliaforms and from mammals [see diagnosis (*15*)].
2. W. A. Clemens, *Zitteliana* **5**, 51 (1980).
3. N. C. Fraser, G. M. Walkden, V. Stewart, *Nature* **314**, 161 (1985).
4. D. Sigogneau-Russell, R. Hahn, *Acta Palaeontol. Pol.* **40**, 245 (1995).
5. P. M. Datta, D. P. Das, *Indian Min.* **50** (no. 3), 217 (1996).
6. F. A. Jenkins *et al.*, *Nature* **385**, 315 (1997).
7. S. G. Lucas, Z.-X. Luo, *J. Vertebr. Paleontol.* **13**, 309 (1993).
8. D. M. Kermack, K. A. Kermack, F. Mussett. *Zool. J. Linn. Soc.* **47**, 407 (1968).

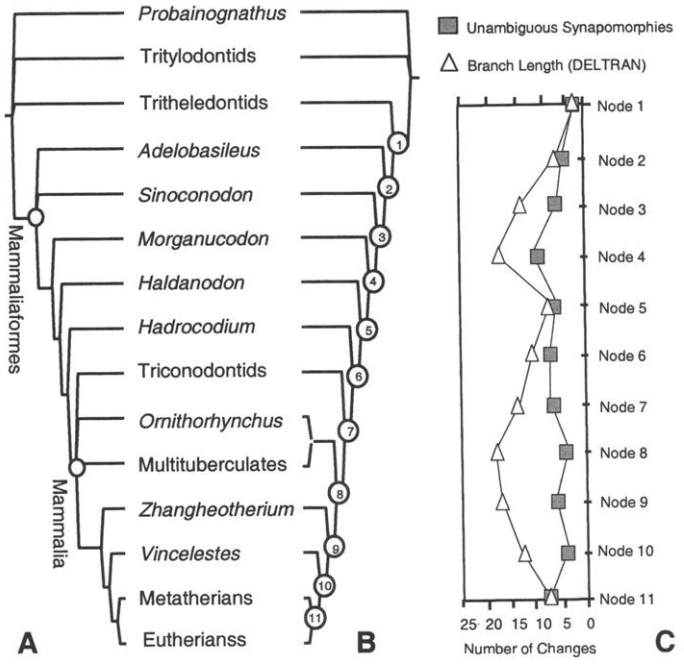

Fig. 4. Phylogenetic relationships of *Hadrocodium* to Mammaliaformes [sensu (*42*), traditional concept of "Mammalia"] and Mammalia [sensu (*42*), mammalian crown group]. (**A**) Preferred tree based on the strict consensus from nine equally parsimonious trees (EPT) from PAUP (4.*) search (branch and bound) of 90 characters that can be coded for *Hadrocodium* (*22*); all multistate characters were unordered in this search. Triconodontids, *Ornithorhynchus*, and multituberculates form an unresolved polytomy, a better resolution of which may require additional cranial and postcranial data beyond the scope of this study, as shown by others (*29*, *30*, *40*). (**B**) An EPT tree from the search with unordered multistate characters. This is identical to the single most parsimonious tree from the branch and bound search with ordered multistate characters. (**C**) Acquisition of mammalian characters in mammaliaform evolution [nodes labeled in (B)]. Squares, unambiguous synapomorphies for each node [the most conservative estimate of character changes (*43*)]; triangles, total number of character changes based on decelerated transformation (DELTRAN) of PAUP [following (*43*)]. Four unambiguous synapomorphies may be diagnostic of the crown-group Mammalia (node 8), below the average of other mammaliaform nodes. The acquisition of mammalian apomorphies occurs incrementally through the mammaliaform-mammal transition, extending a similar evolutionary pattern in nonmammaliaform synapsids (*24*, *25*, *43*) into the evolution of living mammals.

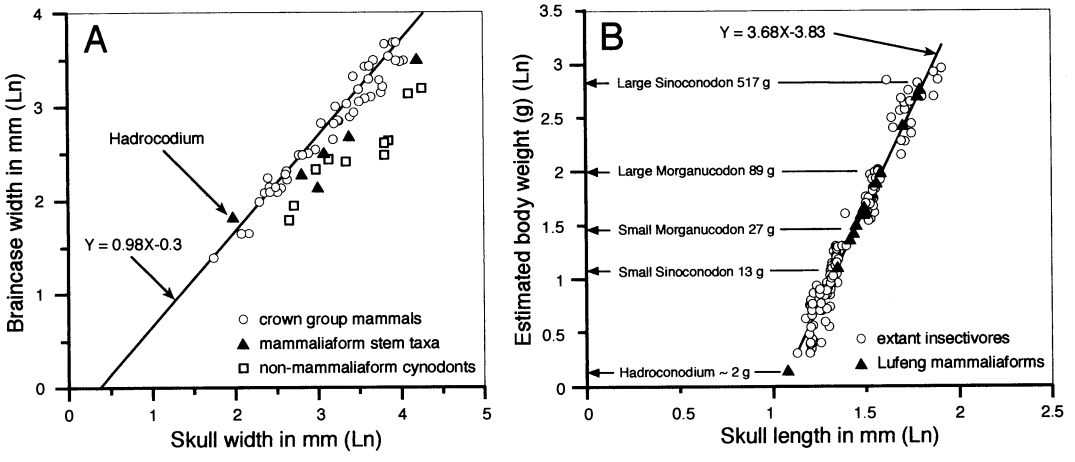

Fig. 5. (**A**) Scaling of brain vault size (width measured at the level of anterior squamosal/parietal suture) relative to skull size (measured at the distance between the left versus right temporomandibular joints). This shows that allometry of small size of *Hadrocodium*, by itself, is not sufficient to account for its very large braincase. *Had-rocodium's* brain vault is larger (wider) than expected for the crown-group mammals with similar skull width from the allometrical regression. By contrast, all contemporaneous mammaliaforms (triangles: *Sinoconodon*, *Morganucodon*, and *Haldanodon*) with the postdentary trough and meckelian groove have smaller (narrower) brain vaults than those living mammal taxa (and *Hadrocodium*) of comparable skull size. The brain vault is narrower in nonmammaliaform cynodonts (squares: *Chaliminia*, *Massetoganthus*, *Probelesodon*, *Probainognathus*, and *Yunnanodon*) than in mammaliaform stem taxa and much narrower than expected for crown group mammals of similar size. The allometric equation (natural logarithmic scale) for the brain vault width (Y) to the skull width at the level of TMJ (X) for species in the mammalian crown groups (circles: 37 living and 8 fossil species): $Y = 0.98X - 0.31$ ($R^2 - 0.715$). Data from cynodonts, mammaliaforms, and *Hadrocodium* are added secondarily for comparison with the regression of extant and fossil species of mammalian crown group. (**B**) Estimated body-size distributions of mammaliaform insectivores in the Early Jurassic Lufeng fauna [following method of Gingerich (*50*)]. The estimated 2-g body mass of *Hadrocodium* is in strong contrast to its contemporary mammaliaforms of the Late Triassic and Early Jurassic, such as *Sinconodon* (from ~13 to ~517 g, based on skull length from 22 to 62 mm) and *Morganucodon* (from 27 to 89 g, based on skull length from 27 to 38 mm). This wide range of body sizes indicates a trophic diversity in the paleoguild of triconodont-like insectivores (*53*, *54*) in the Lufeng mammaliaform fauna.

9. K. A. Kermack, F. Mussett, H. W. Rigney, *Zool. J. Linn. Soc.* **53**, 87 (1973).
10. K. A. Kermack, F. Mussett, H. W. Rigney. *Zool. J. Linn. Soc.* **71**, 1 (1981).
11. A. W. Crompton, *Bull. Brit. Mus. Nat. Hist. Geol.* **24**, 399 (1974).
12. F. R. Parrington, *Philos. Trans. R. Soc. London Ser. B* **282**, 177 (1978).
13. F. A. Jenkins Jr., A. W. Crompton, W. R. Downs, *Science* **222**, 1233 (1983).
14. A. W. Crompton, Z.-X. Luo, in *Mammal Phylogeny*, F. S. Szalay, M. J. Novacek, M. C. McKenna, Eds. (Springer-Verlag, New York, 1993), pp. 30–44.
15. Diagnosis: Dental formula: I5.C1.P2.M2/i4.c1.p2.m2. Each molar has three main cusps and two accessory cuspules in alignment on the laterally compressed crown. Primary lower cusp a occludes in the embrasure between the opposite upper molars (Fig. 1). It differs from *Morganucodon* (*2*, *9*–*14*), *Erythrotherium* (*11*), *Dinnetherium* (*13*), *Haldanodon* (*23*), and triconodontids (*28*, *29*), in which the primary cusp a of the lower molar occludes between cusps A and B of the upper. It differs from *Megazostrodon* (*11*) in lacking prominent labial cingulid cuspules of the upper and from kuehneotheriids (*3*, *4*, *8*) in lacking the triangulation of molar cusps. It differs from morganucodontids, eutriconodonts, and kuehneotheriids in the presence of a much larger postcanine diastema. It differs from *Sinoconodon* (*14*) and most cynodonts in the one-to-one precise occlusion of the upper and lower molars. It lacks the multicuspate rows on the teeth of *Haramiyavia* (*6*), multituberculates (*35*, *36*), and the multiple-ridged teeth of docodonts (*23*). *Hadrocodium* differs from eutriconodonts, multituberculates, symmetrodonts, and all known mammaliaforms in having many derived and distinctive features of mandibular and temporomandibular joints, as described in the text.
16. H.-J. Kuhn, *Abh. Senckenb. Naturforsch. Ges. Frankfurt* **528**, 1 (1971).
17. U. Zeller, *Abh. Senchenb. Naturforsch. Ges. Frankfurt* **545**, 1 (1989).
18. _____, in *Mammal Phylogeny*, F. S. Szalay, M. J. Novacek, M. C. McKenna, Eds. (Springer-Verlag, New York, 1993), pp. 95–107.

19. W. von Maier, *Z. Zool. Syst. Evolutionsforsch.* **27**, 149 (1989).
20. _____, in *Mammal Phylogeny*, F. S. Szalay, M. J. Novacek, M. C. McKenna, Eds. (Springer-Verlag, New York, 1993), pp. 165–181.
21. U. Zeller, in *Morphogenesis of the Mammalian Skull*, H.-J. Kuhn, U. Zeller, Eds. (Parey, Hamburg, 1987), pp. 17–50.
22. Supplementary data are available on *Science* Online at www.sciencemag.org/cgi/content/full/292/5521/1535/DC1.
23. J. A. Lillegraven, G. Krusat, *Contrib. Geol. Univ. Wyom.* **28**, 39 (1991).
24. T. S. Kemp, *Mammal-Like Reptiles and Origin of Mammals* (Academic Press, London, 1982), pp. 1–363.
25. J. A. Hopson, H. R. Barghusen, in *The Ecology and Biology of Mammal-Like Reptiles*, N. Hotton III, P. D. MacLean, J. J. Roth, E. C. Roth, Eds. (Smithsonian Institution Press, Washington, DC, 1986), pp. 83–106.
26. E. F. Allin, J. A. Hopson, in *The Evolutionary Biology of Hearing*, D. B. Webster, R. R. Fay, A. N. Popper, Eds. (Springer-Verlag, New York, 1992), pp. 587–614.
27. Z.-X. Luo, in *In the Shadow of Dinosaurs—Early Mesozoic Tetrapods*, N. C. Fraser, H.-D. Sues, Eds. (Cambridge Univ. Press, Cambridge, 1994), pp. 98–128.
28. R. L. Cifelli, J. R. Wible, F. A. Jenkins Jr., *J. Vertebr. Paleontol.* **18**, 237 (1998).
29. Q. Ji, Z.-X. Luo, S.-A. Ji, *Nature* **398**, 326 (1999).
30. Y.-M. Hu, Y.-Q. Wang, Z.-X. Luo, C.-K. Li, *Nature* **390**, 137 (1997).
31. Z. Kielan-Jaworowska, *Lethaia* **29**, 249 (1997).
32. _____, *Contrib. Geol. Univ. Wyom.* **3**, 21 (1986).
33. T. Rowe, *Science* **273**, 651 (1996).
34. H. J. Jerison, *Evolution of the Brain and Intelligence* (Academic Press, New York, 1973).
35. G. Hahn, *Palaeovertebrata* **18**, 155 (1988).
36. Z. Kielan-Jaworowska, J. H. Hurum, *Acta Palaeontol. Pol.* **42**, 201 (1997).
37. A. M. Musser, M. Archer, *Philos. Trans. R. Soc. London Ser. B* **353**, 1063 (1998).
38. Z.-X., Luo, A. W. Crompton, S. G. Lucas, *J. Vertebr. Paleontol.* **15**, 113 (1995).
39. J. R. Wible, J. A. Hopson, in *Mammal Phylogeny*, F. S. Szalay, M. J. Novacek, M. C. McKenna, Eds. (Springer-Verlag, New York, 1993), pp. 45–62.
40. G. W. Rougier, J. R. Wible, J. A. Hopson, *Am. Mus. Novitates* **3183**, 1 (1996).
41. Z.-X. Luo, A. W. Crompton. *J. Vertebr. Paleontol.* **14**, 341 (1994).
42. T. Rowe, *J. Vertebr. Paleontol.* **8**, 241 (1988).
43. C. A. Sidor, J. A. Hopson, *Paleobiology* **24**, 254 (1998).
44. The negative allometry of the middle ear bones relative to the whole skull during development of *Monodelphis* is consistent with the observation of monotremes and some eutherians. During the development of *Ornithorhynchus* (*17*, *18*), the malleus shows negative allometry relative to the overall growth of the entire skull. As the posterior Meckel's cartilage is ossified and transformed into the malleus, the diameter of the arc between the anterior process of the malleus and the manubrium increases by only 25% (from 3 to ~4 mm) as the skull length increases by almost 300% (from 24 to 106 mm). The placental *Tupaia* (*21*) has a substantial growth in skull size after the ossification and fixation of size of the middle ear structure.
45. S. Nummela, *Theor. Biol.* **4**, 387 (1997).
46. K. K. Smith, *Evolution* **51**, 1663 (1997).
47. Differentiation of the central nervous system in eutherians (*21*, *46*) occurs in advance of the ossification of TMJ, which, in turn, occurs before the ossification of middle ear ossicles (*21*, *46*). The sequence of these events is the opposite that of marsupials, indicating an unambiguous case of heterochrony among living therians [(*46*), and references cited therein]. The dentary/squamosal joint is also established earlier than ossification of the middle ear ossicles in monotremes (*16*–*18*), similar to placentals but different from marsupials [(*19*, *20*) and references cited therein]. The Meckel's cartilage and its derivative elements (the incus and malleus) are positioned on the basicranium and well separated from the dentary in early ontogeny in eutherians (*21*). This is different from marsupials, in which the Meckel's cartilage and its derivative elements are closely attached to the dentary until the final separation from the latter in a later postnatal stage (*19*, *20*).
48. S. W. Herring, *Am. Zool.* **33**, 472 (1993).
49. Teratological evidence shows that masticatory muscle attachment to the Meckel's cartilage in abnormal human development can delay its reabsorption (*48*). Thus, reabsorption of the Meckel's cartilage may be associated with the loss of mechanical stress and loading as the masticatory muscles shifted their attachment from Meckel's cartilage to the dentary during normal development (*48*). Maier (*19*, *20*) also proposed that movement of the dentary during suckling would result in disruption of the Meckel's cartilage.
50. P. D. Gingerich, B. H. Smith, in *Size and Scaling in Primate Biology*, W. L. Jungers, Ed. (Plenum, New York, 1984), pp. 257–272.
51. J. I. Bloch, K. D. Rose, P. D. Gingerich, *J. Mammal.* **79**, 804 (1998).
52. J. Alroy, *Science* **280**, 731 (1998).
53. B. Van Valkenburgh, *Trends Ecol. Evol.* **10**, 71 (1995).
54. J. Jernvall, J. P. Hunter, M. Fortelius, *Science* **252**, 1831 (1996).
55. M. Foote, *Annu. Rev. Ecol. Syst.* **28**, 129 (1997).

56. We thank W. W. Amaral for a superb preparation; M. Klingler for graphics; J. Suhan for photography; A. Henrici for assistance; F. A. Jenkins, J. R. Wible, G.-H. Cui, and F.-K. Zhang for access to the comparative collections; P. D. Gingerich for generously providing body mass/skull measurements of extant insectivores; J. Alroy, K. C. Beard, M. R. Dawson, P. D. Gingerich, Z. Kielan-Jaworowska, T. Rowe, K. K. Smith, J. G. M. Thewissen, and J. R. Wible for discussion; and M. R. Dawson, J. A. Hopson, Z. Kielan-Jaworowska, and J. R. Wible for improving the paper. Research supported by the CAREER award of NSF (DEB 95278902), National Geographic Society (grant 5338-94), and Carnegie Museum (Z.-X.L), and NIH and Harvard University (A.W.C.).

20 December 2000; accepted 15 March 2001

Chromatin Docking and Exchange Activity Enhancement of RCC1 by Histones H2A and H2B

Michael E. Nemergut,[1,2]*† Craig A. Mizzen,[4] Todd Stukenberg,[4] C. David Allis,[4] Ian G. Macara[1,3]

The Ran guanosine triphosphatase (GTPase) controls nucleocytoplasmic transport, mitotic spindle formation, and nuclear envelope assembly. These functions rely on the association of the Ran-specific exchange factor, RCC1 (regulator of chromosome condensation 1), with chromatin. We find that RCC1 binds directly to mononucleosomes and to histones H2A and H2B. RCC1 utilizes these histones to bind *Xenopus* sperm chromatin, and the binding of RCC1 to nucleosomes or histones stimulates the catalytic activity of RCC1. We propose that the docking of RCC1 to H2A/H2B establishes the polarity of the Ran-GTP gradient that drives nuclear envelope assembly, nuclear transport, and other nuclear events.

RCC1 can be considered as a chromatin marker. Catalysis of guanine nucleotide exchange on Ran by RCC1 to produce Ran-GTP is essential for mitotic spindle assembly and nuclear envelope formation (*1*–*4*). Once enclosed by the envelope, chromatin-bound RCC1 generates a Ran-GTP gradient across nuclear pores that permits vectorial nucleocytoplasmic transport (*4*). The docking mechanism for RCC1 onto chromatin is unknown. RCC1 may bind DNA in vitro, but removal of the NH_2-terminal domain of

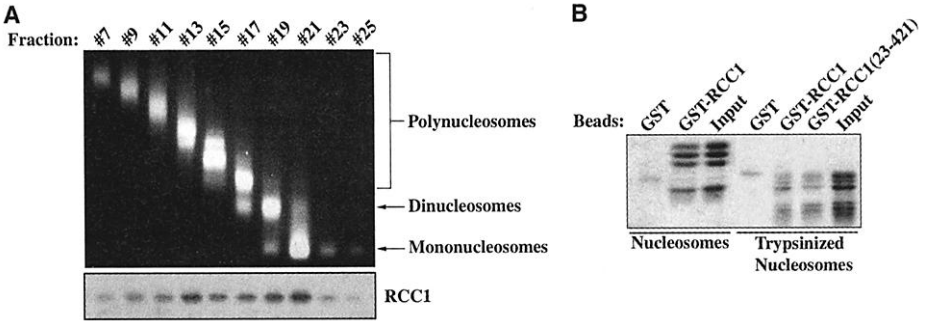

Fig. 1. RCC1 binds mononucleosomes. (**A**) HeLa nuclei were digested with micrococcal nuclease and centrifuged through a linear 8 to 20% sucrose gradient. Samples of individual fractions were electrophoresed through a tris-borate EDTA-agarose gel and visualized by ethidium bromide staining (top) or precipitated with trichloroacetic acid, subjected to SDS-PAGE, and immunoblotted (N-19, Santa Cruz) for endogenous RCC1 (bottom). (**B**) Immobilized GST, GST-RCC1, or GST-RCC1(23-421) was incubated with intact or trypsinized H1-depleted mononucleosomes. After washing, proteins were eluted, subjected to SDS-PAGE, and stained with Coomassie.